ERM

75 Valley Stream Parkway
Suite 200
Malvern, PA
19355

Telephone: +1 484 913 0300

www.erm.com

Technical Memo

Date	1 March 2023
Reference	ERM Project #0623691: Bandwidth IG, LLC San Francisco Bay
Subject	Scour / Erosion Analysis and Climate Change Effects

1. INTRODUCTION

The California State Lands Commission would like to understand the impact of climate change on the scouring potential of a proposed fiber optic cable that will be buried 3 to 6 feet below the San Francisco Bay bed. An analysis was performed at two critical points along the cable route, specifically near the two shallow regions at the ends of the cable route: near Brisbane on the east and San Leandro on the west. Two approaches were used: an evidence-based approach, and a model-based approach.

The previous field studies conducted during the cable route planning related to sediment bed characterization and near-bed current velocities were used to understand the baseline (current conditions) scouring potential for a buried cable. In addition to the measured velocities, some of the extreme events that occurred historically in the region and associated estimation of near-bed velocities were examined for any exacerbation of sediment scouring at the two critical locations.

The same methodology was then applied for evaluating the effect of climate change on projected wind speeds and associated currents and wave-induced near-bed velocities on the change in the scouring potential. A business-as-usual worst-case climate scenario was used to obtain the relevant variables needed for this study.

The sediment scouring analysis was performed for the present conditions and the future year 2050. Projected currents and wave fields for SF Bay were identified from USGS COSMOS (Coastal Storm Modeling System) SF Bay model[1]. Wave fields for historical storm frequencies of 1, 20 and 100 years were identified from OCOF (“Our Coast Our Future”) web tool[2].

2. METHODOLOGY

The study area is provided in Figure 1, showing the planned cable route across San Francisco Bay and the east and west critical locations where this study was focused.

[1] Downscaling wind and wavefields for 21st century coastal flood hazard projections in a region of complex terrain - O'Neill - 2017 - Earth and Space Science - Wiley Online Library

[2] Hazard Map – Our Coast, Our Future (ourcoastourfuture.org)

Figure 1: Study Area

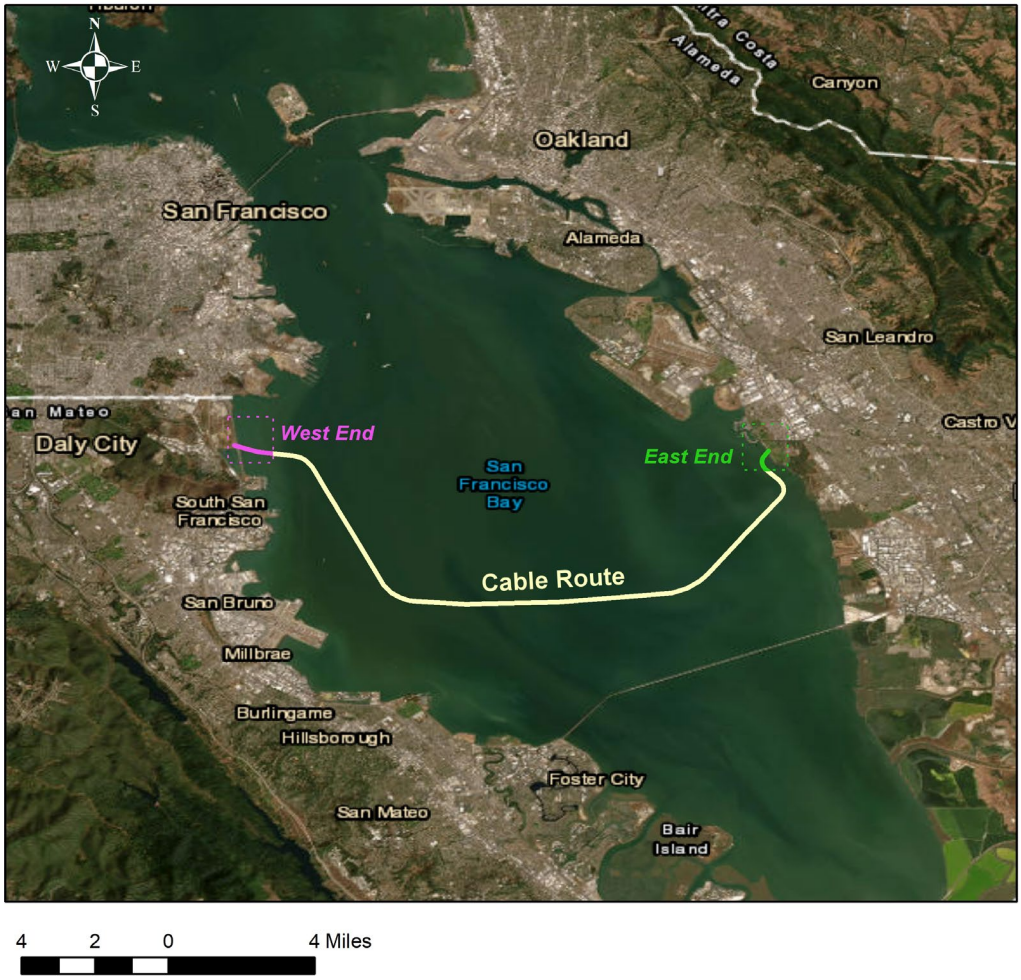

3. EVIDENCE-BASED APPROACH

3.1 Review of Historic Bathymetric Surveys in South Bay

According to U.S. Geological Survey analyses of San Francisco Bay (Jaffe and Foxgrover 2006[a] and 2006[b]), between 1956 to 2005 there was a net erosion in the eastern shore's shallow area (i.e. region less than 1 meter deep) in the section north of Dumbarton Bridge where the cable route is planned. Erosion decreased from 1983 to 2005 during a period of net deposition in areas within the center of the bay, and along the ship channel, possibly due to increased sediment loads from the Central Bay area. On the eastern end of the cable route, there was some loss of intertidal mud flats between 1956 and 1983, in addition to the construction of docks and expansion of the Oakland International Airport. The coastal morphology between 1956 and 2005 remained the same with some additional loss of mud flats. However, the shoreline south of the cable route did shift eastward over time, making the coastline's profile more smooth (See Figures 2 to 5).

Figure 2: San Francisco Bay Sedimentation 1956, 1983, and 2005

Based on Jaffe and Foxgrover 2006[b]

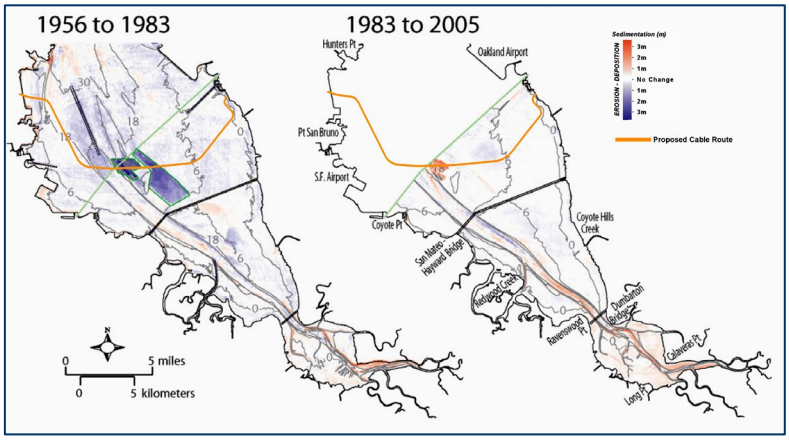

Figure 3: San Francisco Bay Bathymetry 1956, 1983, and 2005

Based on Jaffe and Foxgrover 2006[a]

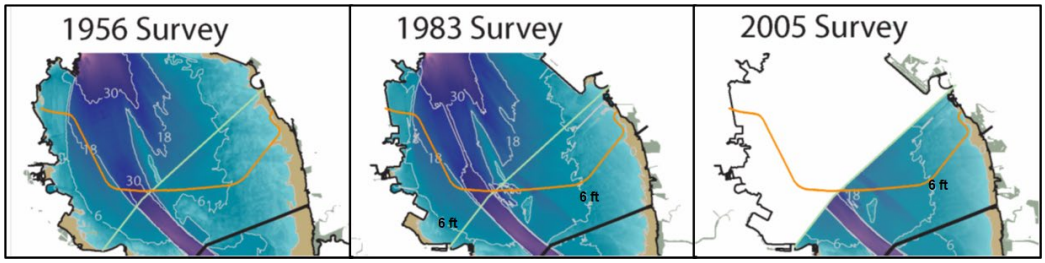

Figure 4: East San Francisco Bay Bathymetry 1956, 1983, and 2005

Based on Jaffe and Foxgrover 2006[a]

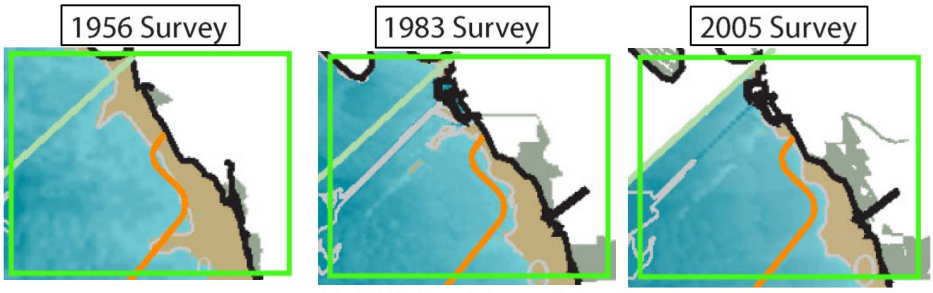

Figure 5: West San Francisco Bay Bathymetry 1956 and 1983

Based on Jaffe and Foxgrover 2006[a]

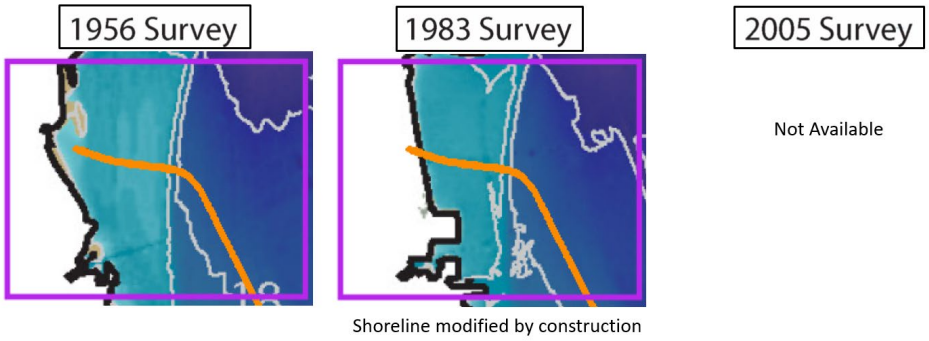

The bathymetry of the South Bay mostly changed in the ship channel and along the coastlines. The 6 ft contour line extent mostly remains stable based on Figures 2 to 6. This means if there is any buried cable 3 ft to 6 ft below the bay sediment bed near the west and east ends it will not be subjected to any type of extreme erosion that exposes the buried cable. From 1956 to 2005, the bay bed near the shoreline seems to be stable despite various types of storm events that happened during the period 1956 to 2005.

The intertidal flat changes are shown in Figure 6. Near the west and east ends of the proposed cable route, there is no intertidal flat loss or gain.

Figure 6: Study Area Overlaid on the Intertidal Flat Changes Map

Based on Jaffe and Foxgrover 2006[a]

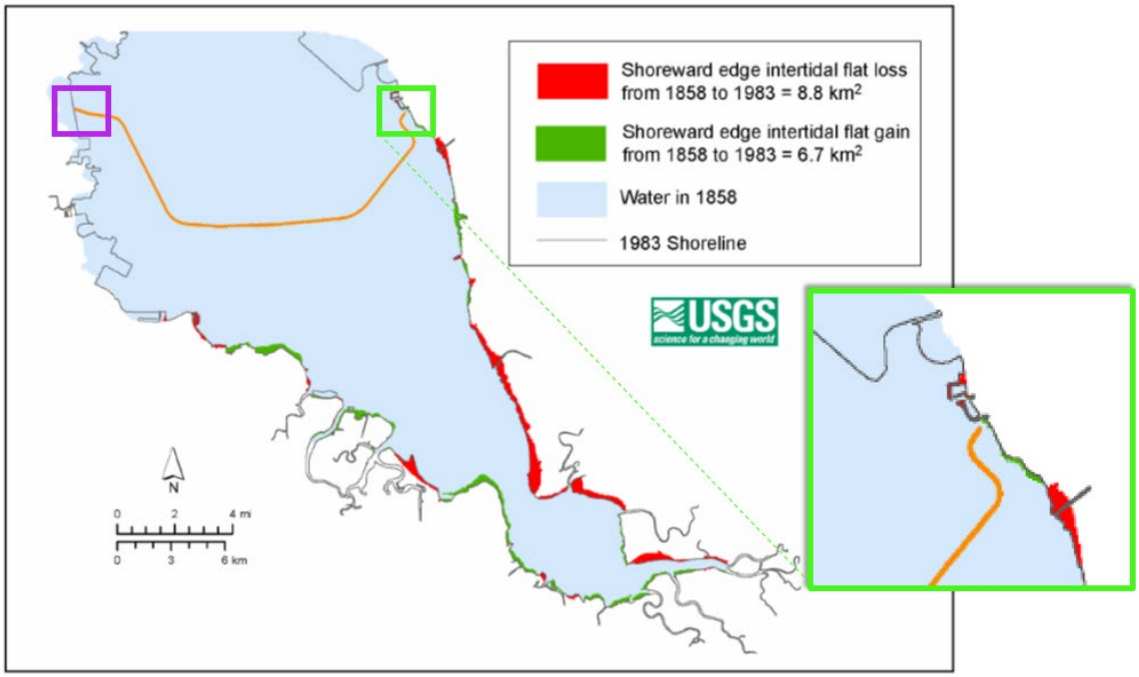

3.2 Overview of Sediment Transport in the San Francisco Bay

ERM reviewed a technical paper published in Science Direct by Barnard et al., 2013 to get an understanding of sediment transport in the San Francisco Bay. According to this paper, while most other regions of the bay lost sediments, South Bay gained sediments of about 11 million m3 during the period 1983-2005 (See Figure 7). The historical sources of sediments in the Bay are:

1) Load from the Delta (Sacramento and San Joaquin Rivers)

2) Reduced sediment load due to the construction of dams, reservoirs, flood control, stream bank protection, and shoreline armoring due to the late 1800s gold rush

3) Delta modifications due to reduced suspended sediments, sediment removal due to dredging and bay fill due to subsidence and sea level rise

The following factors affect sediment transport in the Bay.

1) Wet and dry season variability

2) Freshwater inflow annual variability

3) Seasonal wind strength variability

Figure 7: Sediment losses/gains in the San Francisco Bay

The current conditions in the South Bay that affect sediment transport include:

- Spring tidal currents are typically 0.4 m/s on the shoals
- Strong winds are typical of summer sea breezes and winter storms (~16 mph), generating waves and sediment resuspension
- Bottom currents are slower than the other parts of the Bay
- Wind waves are important for cohesive sediment resuspension on shoals
- Large sediment fluxes occur from a combination of wind waves and tidal currents
- Both the east and west ends of the cable route did not show strong evidence of historical coastal area erosion or deposition

With Climate Change

- Increase the frequency of extreme water level events
- Cause higher precipitation peaks earlier in the season, weaker snow-melt
- Impact circulation patterns

- Shift peak sediment loads earlier in the year
- Increase the frequency of coastal flooding events
- Decline in suspended sediment concentration
- Wetlands will need more sediment load to compete with sea level rise

3.3 Cohesive Sediment Erosion Study in South Bay

A team of scientists from Stanford University and Integral Consulting (Egan et al. 2020) conducted a field study in the South Bay to understand the mechanisms driving cohesive sediment erosion due to the combined effect of waves and currents in a shallow region. The study locations are shown in Figure 8.

Figure 8: Study Locations

The depths at P1 and P2 are 1.5 m and 0.5 m, respectively, which are similar to the depths we find in the west and ends of the proposed cable route. The study involved three 4-week periods:

- July 17, 2018 – August 15, 2018 (summer deployment)
- January 10, 2019 – February 7, 2019; (winter deployment)
- April 17, 2019 – May 15, 2019 (spring deployment)

A one week period time series of data plotted in Figure 9 shows the variation of orbital velocities in the order of 5 to 30 cm/sec resulting in both erosion and deposition with a +/- 0.5 cm change in the bed level.

Figure 9: Seven-day time series during the spring deployment showing Vectrino measurements of (a) the bottom wave-orbital velocity, u_b, (b) the erosive sediment flux magnitude of the fluctuating bed level, |E|, (c) the changes in the bed level thickness, z_b

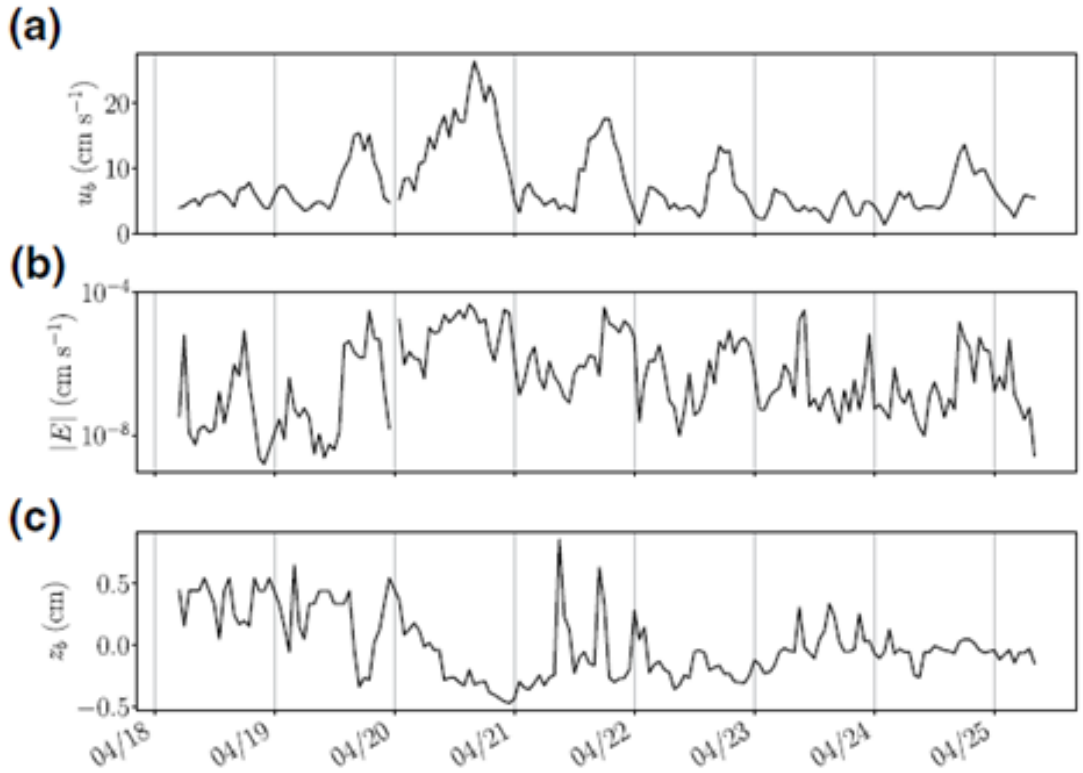

The critical cohesive shear stress measurements shown in Table 1 vary for different seasons and locations which affects the erosion potential. The term r^2 refers to the least square fit between sedflume and field data measurements.

Table 1: Critical Cohesive Erosion Stress (Pa)

	Critical Erosion Shear Stress (Pa) (r^2 in parentheses)		
Location	**Summer**	**Winter**	**Spring**
P1	1.4 (0.54)		0.79 (0.64)
P2	9.04 (0.02)	0.16 (0.33)	0.3 (0.10)
Vec	0.45 (0.30)		0.15 (0.35)

The study concluded that waves effectively erode sediments into a thin region near the bed, allowing tidal currents to distribute the sediments through the rest of the water column in shallow regions. However, cycles of erosion and deposition happen to result in minimal bed level changes and do not lead to continuous erosion leading to scouring.

4. MODEL-BASED APPROACH

A sediment transport model, Sedtrans05, was applied to examine the potential changes in sediment transport at the two critical end locations on the cable route.

Sedtrans05 (Neumeier et al., 2008) provides computations to estimate sediment transport of both cohesive and non-cohesive sediments as a function of currents, weaves, water depth, and

sediment type. The Cohesive Sediment Algorithm (CSA) in the model is appropriate for water with salinity above 10 to 15 ppt. However, the CSA does not include movement due to biological processes such as bioturbation, lateral movement of fluid mud, the resuspension of fluid mud by waves, or the effects of Holmboe waves at the water-sediment interface.

4.1 Model Inputs

Model inputs gathered for this analysis included San Francisco Bay currents, salinity, water temperature, wave data, and sediment characteristics.

4.1.1 Waves and Currents

Waves and currents were measured (A2Sea 2022) in the deeper section of the proposed route using by Acoustic Doppler Current Profiler (ADCP) at a location shown in Figure 10. Waves and currents were measured from July 20, 2022 through August 24, 2022. Wave information was recorded every 40 minutes, while current speeds and directions were recorded every 10 minutes. Statistical analysis of currents and waves were performed to understand the current and wave characteristics near the proposed route. Figure 11 shows tidal currents are predominately in the northwest and southeast direction. Figure 11 also shows the plots of wave height with wave period and wave direction. Large wave heights in the range of 10 to 70 cm have wave periods in the range of 3 to 6 secs while small wave heights in the range of 1 to 2 cm have wave periods in the range of 12 to 30 secs. Wave heights are distributed across all directions at the proposed route. Currents and waves obtained from field measurements were measured at a deeper location in the Bay and hence they were downscaled to represent currents and waves in the east and west ends using COSMOS model results (See Table 3 and Table 4).

Figure 10: ADCP Location

Figure 11: Currents and Waves at the Proposed Route

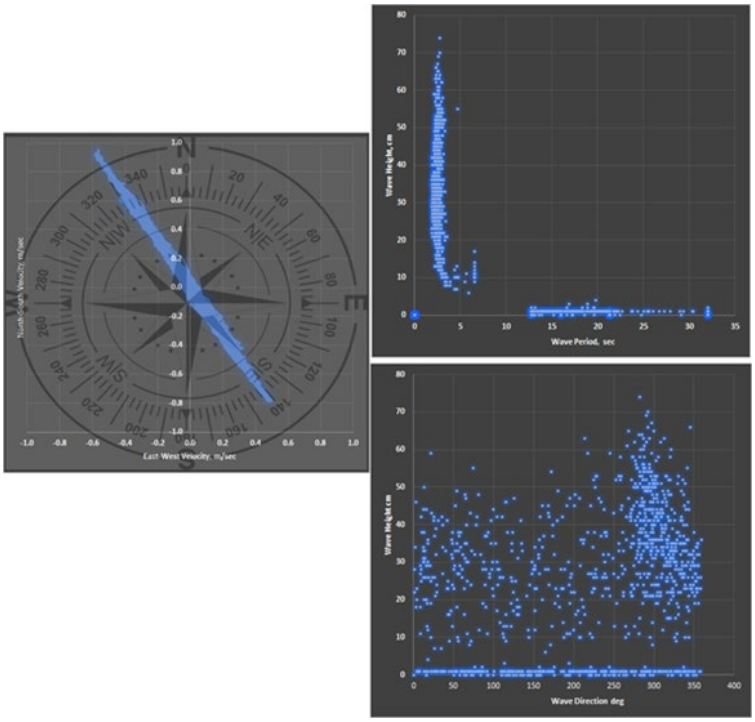

The percent occurrence in a day of various wave heights is shown in Table 2.

Table 2: Percent Occurrence in a Day of Various Wave Heights

Wave Height Bins (m)	% Occurrence in a Day
0.0 – 0.1	37
0.1 – 0.2	7
0.2 – 0.3	17
0.3 – 0.4	17
0.4 – 0.5	12
0.5 – 0.6	7
0.6 – 0.7	2
0.7 – 0.8	0

Table 2 shows that 44% of the time, wave heights are less than 20 cm while 46% of the time wave heights are between 20 to 50 cm. Wave heights > 50 cm occur 10% of the time in a day. This clearly shows while larger wave heights can cause erosion, smaller wave heights promote deposition.

The waves and currents statistics for current conditions and the future year 2050 are shown in Table 3 and Table 4, respectively.

Table 3: Currents

Measurements	Currents Magitude m/sec			
ADCP Location	Surface	Mid Depth (5.62 m)	1 meter above bottom (10.62 m)	Bottom (11.62 m)
Min	0.001	0.002	0.003	0.002
Max	0.883	1.104	1.243	0.892
Avg	0.311	0.379	0.390	0.300
Left Coast - Computed using COSMOS model results				
Min	0.00035			
Max	0.31332			
Avg	0.11048			
Right Coast - Computed using COSMOS model results				
Min	0.00044			
Max	0.38867			
Avg	0.13704			
COSMOS - Our Coast of the Future				
Year	SLR cm	Annual RP Currents m/sec	20 Year RP Currents m/sec	100 Year RP Currents m/sec
Left Coast				
2021	25	0.339	0.252	0.775
2050	75	0.341	0.251	0.792
Right Coast				
2021	25	0.392	0.298	0.458
2050	75	0.423	0.305	0.485
ADCP Location				
2021	25	0.956	0.913	0.911
2050	75	0.961	0.903	0.902

Table 4: Waves

Measurements				
ADCP Location	Wave Height m	Peak Period secs	Mean Period secs	Mean Direction deg
Min	0.01	2	1.9	1
Max	0.74	25.6	32	359
Avg	0.216	5.49	6.06	284.5
Left Coast				
Min	0.004			
Max	0.263			
Avg	0.077			
Right Coast				
Min	0.001			
Max	0.093			
Avg	0.027			
COSMOS - Our Coast of the Future				
Year	SLR cm	Annual RP Wave Height cm	20 Year RP Wave Height cm	100 Year RP Wave Height m
Left Coast				
2021	25	0.475	0.628	0.832
2050	75	0.512	0.841	0.869
Right Coast				
2021	25	0.875	0.919	0.924
2050	75	0.879	1.053	1.054
ADCP Location				
2021	25	1.264	0.997	1.686
2050	75	1.317	1.022	1.701

Climate change wave heights and currents were obtained from COSMOS[3]. Annual storm frequency results in Table 3 show that the maximum wave heights at the west end, east end, and field measurement locations along the cable route increase by about 7%,1% and 4%, respectively. Similarly, annual storm frequency results in Table 4 show the maximum currents at the west end, east end, and field measurement locations along the cable route by about 1%, 8% and 1%,

[3] Hazard Map – Our Coast, Our Future (ourcoastourfuture.org)

respectively. Another study by O'Neill (2017) on downscaling of wind and wavefields for 21st-century coastal flood hazard projections in the San Francisco Bay shows that there is not much variation in the maximum and average wave heights in the South Bay between the period 1975-2004 and 2010-2100 (See Table 5). This means climate change shows a minimal change in the wave heights and currents in the South Bay and should not exacerbate erosion along the proposed route.

Table 5: Climate Change Projects (O'Neil 2017)

Time Period	Maximum Wave Height (m)	Average Wave Height (m)
1975 – 2004	1.05	0.57
2010 - 2100	1.04	0.55

4.1.2 Sediment Characteristics

Bed Characterization along the cable route (A2Sea 2022) is shown in Figure 12. The sediment bed type at the west end is clay while it is clay/sand type at the east end. The sediment grain size information was obtained from a sediment core study conducted in the South Bay by USGS (Woodrow et al. 2014). The sediment core locations are shown in Figure 13. The sediment core information at Sample ID 151 shown in Figure 13 was selected since it is inside the 6 ft contour line that can represent the bed conditions at both the east and west ends. A mass-weighted average of sediment samples that had only clay shown in Table 6 was used to estimate the grain particle size as 1.96131e-06 m (approximately 2 microns). The critical cohesive bed shear stress was obtained from values presented in Table 1. The bottom roughness was obtained from Egan et al. (2020).

Figure 12: Bed Characterization along the Proposed Cable Route

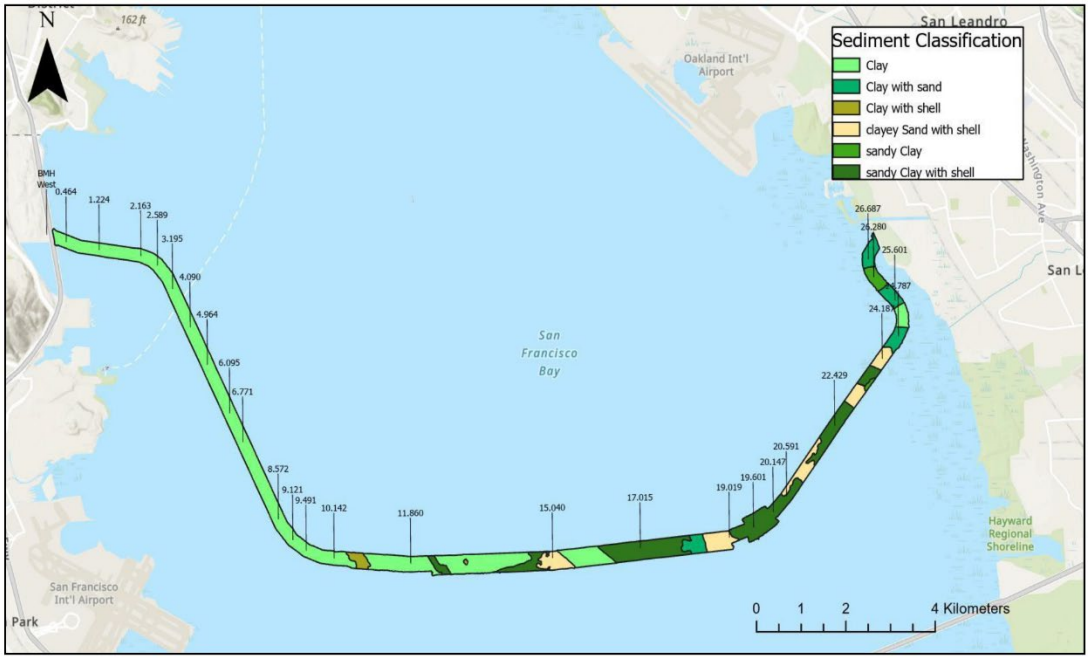

Figure 13: Sediment Core Sample ID 151

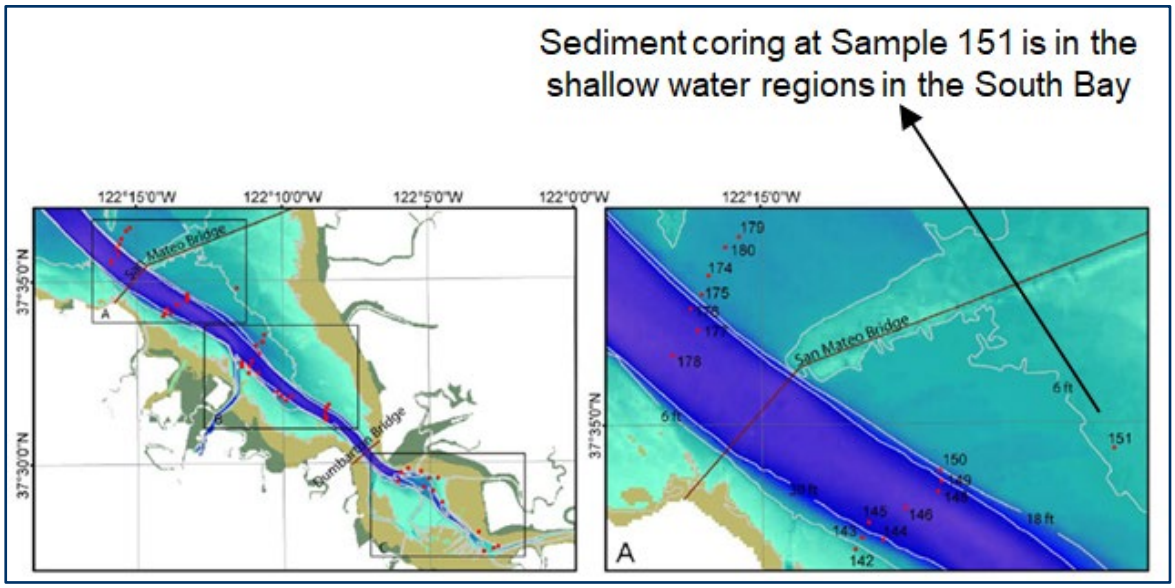

Table 6: Sediment Grain Sizes for Clay Material at Sample ID 151

Sample ID's	Phi % / Clay																	
	8	8.25	8.5	8.75	9	9.25	9.5	9.75	10	10.25	10.5	10.75	11	11.25	11.5	11.75	12	14
Core 90-4(Bottom part) 80-82 cm	3.73	3.60	3.21	3.01	2.75	2.56	2.29	2.10	1.83	1.44	1.44	0.92	0.72	0.39	0.07	0.00	0.00	0.00
Core 90-4(Bottom part) 130-132 cm	1.26	1.17	1.08	0.99	0.90	0.84	0.75	0.68	0.56	0.45	0.45	0.29	0.25	0.18	0.11	0.09	0.07	0.16
Core 90-8A 80-85 cm	4.77	4.48	4.18	3.78	3.58	3.38	3.08	2.78	2.39	1.89	1.89	1.29	1.09	0.80	0.50	0.50	0.30	1.09
Core 90-8B 18-20 cm	5.06	4.76	4.27	3.97	3.57	3.27	3.08	2.88	2.58	1.98	2.18	1.39	1.09	0.60	0.10	0.00	0.00	0.00
Core 90-8B 80-82 cm	5.55	5.25	4.76	4.36	4.06	3.67	3.37	3.07	2.48	1.98	1.98	1.19	1.09	0.79	0.50	0.40	0.40	1.29
Core 90-12(Bottom part) 30-32 cm	4.96	4.58	4.19	3.81	3.43	3.24	3.05	2.76	2.48	1.91	2.10	1.24	1.05	0.57	0.10	0.00	0.00	0.00
Core 90-12(Bottom part) 60-62 cm	1.45	1.40	1.27	1.14	1.00	0.93	0.79	0.71	0.58	0.48	0.48	0.32	0.29	0.21	0.13	0.13	0.08	0.16
Core 90-12(Top part) 28-30 cm	5.04	4.84	4.35	4.05	3.76	3.56	3.16	2.97	2.47	1.88	1.98	1.29	1.09	0.69	0.49	0.40	0.30	0.49
Core 90-23A 82-84 cm	4.85	4.55	4.15	3.76	3.56	3.36	3.07	2.77	2.37	1.88	1.88	1.29	0.99	0.79	0.49	0.40	0.30	0.99
Core 90-23B 10-12 cm	5.65	5.35	4.95	4.56	4.26	3.96	3.77	3.47	3.07	2.48	2.58	1.59	1.29	0.59	0.20	0.00	0.00	0.00
Core 90-38A 38-40 cm	5.13	4.83	4.34	4.04	3.75	3.45	3.16	2.96	2.47	1.87	2.07	1.28	1.18	0.79	0.49	0.49	0.30	1.18
Core 90-38A 100-102 cm	4.96	4.66	4.06	3.77	3.47	3.27	2.87	2.68	2.28	1.68	1.88	1.09	1.09	0.69	0.40	0.40	0.20	0.40
Core 90-38B 20-22 cm	5.07	4.78	4.38	3.98	3.68	3.38	3.08	2.69	2.29	1.89	1.89	1.09	1.09	0.80	0.50	0.40	0.20	0.40
Core 90-142A 37-39 cm	5.33	5.04	4.55	4.17	3.88	3.58	3.20	2.91	2.52	1.94	1.94	1.26	1.16	0.78	0.58	0.39	0.39	1.16
Core 90-142A 130-132 cm	3.59	3.15	2.71	2.45	2.10	1.84	1.58	1.40	1.14	0.88	0.96	0.61	0.61	0.44	0.26	0.26	0.18	0.61
Core 90-142B 20-22 cm	4.05	3.70	3.26	2.99	2.73	2.47	2.20	2.02	1.67	1.32	1.41	0.88	0.79	0.53	0.35	0.26	0.18	0.26
Core 90-142B 45-46 cm	2.64	2.40	2.23	1.99	1.87	1.70	1.58	1.41	1.23	0.94	1.05	0.64	0.64	0.41	0.29	0.29	0.18	0.41
Core 90-142B 47-48 cm	2.21	2.07	1.93	1.79	1.65	1.55	1.41	1.32	1.08	0.89	0.89	0.56	0.47	0.33	0.19	0.19	0.05	0.09
Core 90-146 55-56 cm	0.50	0.47	0.43	0.39	0.35	0.32	0.29	0.27	0.23	0.18	0.19	0.12	0.12	0.08	0.06	0.05	0.03	0.06
Core 90-146 100-102 cm	3.26	3.09	2.66	2.49	2.32	2.15	1.89	1.80	1.46	1.20	1.37	0.77	0.86	0.52	0.43	0.34	0.17	0.26
Core 90-151A 40-42 cm	4.16	3.96	3.66	3.47	3.17	2.97	2.77	2.58	2.18	1.78	1.88	1.19	1.09	0.89	0.50	0.50	0.30	0.50
Core 90-151A 60-65 cm	5.46	5.16	4.67	4.27	4.07	3.67	3.38	2.98	2.58	1.99	1.99	1.19	1.19	0.70	0.50	0.50	0.30	1.29
Core 90-151B 56-58 cm	3.48	3.28	2.88	2.78	2.58	2.39	2.09	1.99	1.69	1.39	1.39	0.89	0.80	0.60	0.40	0.40	0.20	0.40
Core 90-151B 80-85 cm	3.06	2.79	2.52	2.34	2.16	1.98	1.89	1.62	1.44	1.17	1.17	0.81	0.72	0.45	0.36	0.27	0.18	0.27
Core 90-178A 69-70 cm	4.53	4.26	3.83	3.48	3.13	2.87	2.61	2.35	2.00	1.57	1.57	1.04	0.96	0.70	0.44	0.35	0.26	0.70
Core 90-178B 50-52 cm	2.35	2.17	1.94	1.72	1.63	1.40	1.31	1.13	0.99	0.77	0.81	0.50	0.50	0.32	0.23	0.18	0.14	0.23
Core 90-180A 60-62 cm	4.70	4.41	3.83	3.45	3.16	2.78	2.59	2.21	1.92	1.44	1.53	0.96	0.86	0.58	0.38	0.29	0.19	0.48
Core 90-180A 108-110 cm	3.38	2.97	2.73	2.33	2.09	1.85	1.61	1.37	1.21	0.96	0.96	0.64	0.64	0.40	0.32	0.24	0.16	0.40
Core 90-180B 28-30 cm	2.46	2.24	2.01	1.79	1.57	1.45	1.29	1.12	0.95	0.78	0.78	0.50	0.50	0.34	0.22	0.22	0.11	0.17
Core 90-180B 73-75 cm	3.76	3.49	3.04	2.78	2.42	2.24	2.06	1.79	1.52	1.25	1.25	0.90	0.72	0.63	0.36	0.27	0.27	0.27
Core 90-180B 122-124 cm	7.10	6.70	6.00	5.50	5.20	4.80	4.40	4.00	3.30	2.60	2.60	1.50	1.30	0.90	0.50	0.30	0.30	0.90

4.2 Model Analysis

The sedtrans05 model was run for the period 07/16/2022 to 08/22/2022 using the currents (speed and direction) and wave data (wave height, wave period and wave direction) along with sediment bed input parameters described in Section 4.1. Current speeds and wave heights are shown in Figure 13 and currents direction and waves direction are shown in Figure 14. The model-predicted bed level change is shown in Figure 15. Positive values of bed level change represent erosion while the negative values represent deposition. This figure clearly shows cycles of erosion and

deposition during the period of the simulation. The bed level change is also in the same range as the field measurements results shown in Section 3.3. The effective bed shear stress due to the combined action of waves and currents is shown in Figure 15. The bed shear stress varies greater than the critical cohesive shear stress of 2 Pa resulting in erosion based on the field measurements described in Section 3.3.

For various current speeds and directions, erosion increases with wave heights in shallow water. For larger wave heights > 0.25 m, erosion results in a decrease in the bed level in the range of 2 to 5 cm. For smaller wave heights in the range of 0.1 to 0.25 m, deposition of sediments results in the increase of bed level in the range of 2 to 5 cm depending on the availability of suspended sediments. Due to the oscillatory nature of waves at any specific location, cycles of erosion and deposition happen depending on the change in the wave amplitude at a specific location. Field measurements on wave data show that on approximately 45% of any typical day, the wave heights are < 0.2 m, 46% of any typical day it is in the range of 0.2 to 0.5 m and on 9% of any typical day it is > 0.5 m.

Figure 14: Currents and Waves Obtained from Field Measurements and Downscaled to East and West Ends using COSMOS

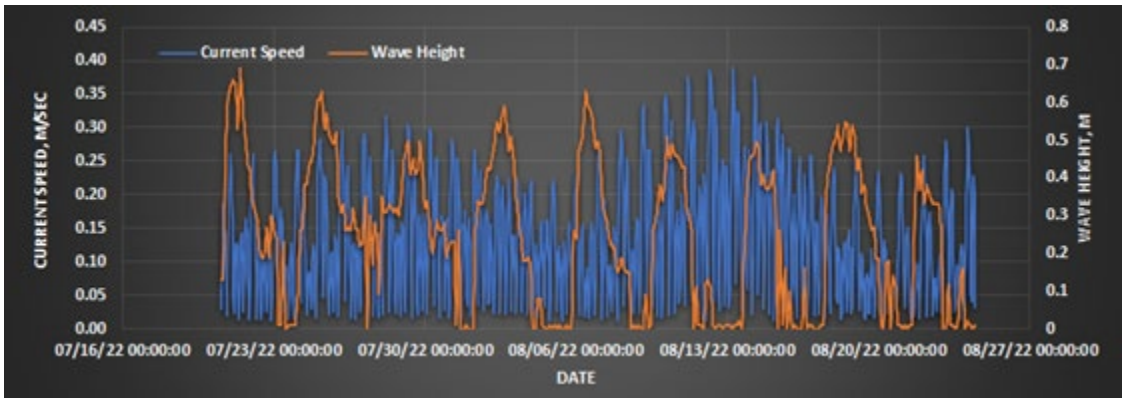

Figure 15: Current and Wave Directions Obtained from Field Measurements

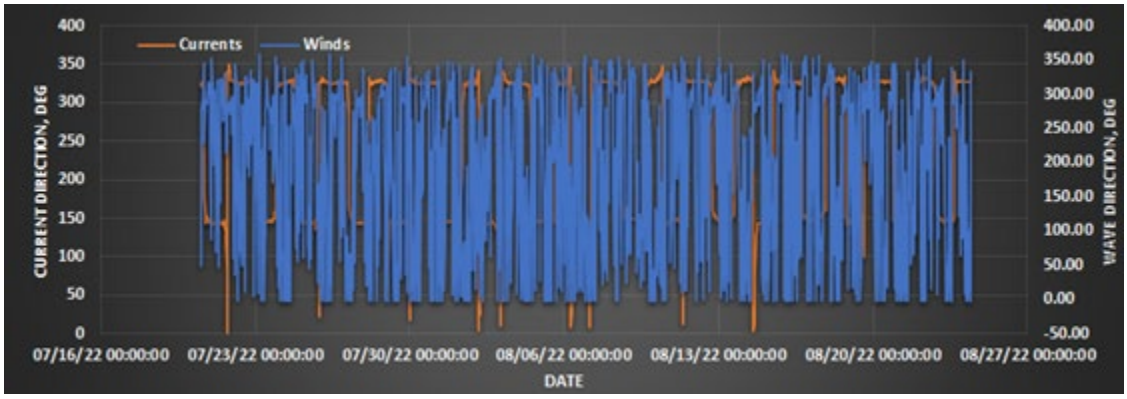

Figure 16: Bed Level Change due to Combined Wave and Current Interaction on the Erosion / Deposition

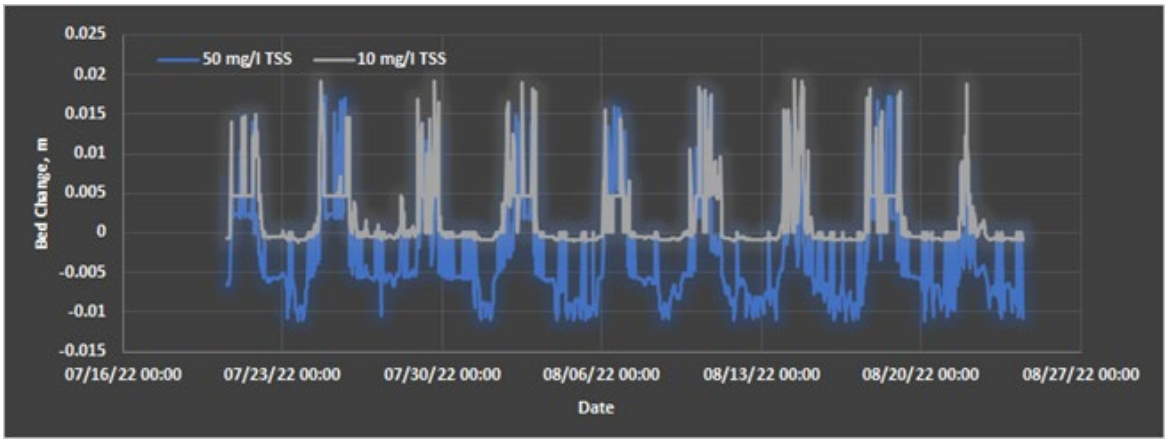

Figure 17: Effective Hydrodynamic Bed Shear Stress due to the Combined Action of Currents and Waves

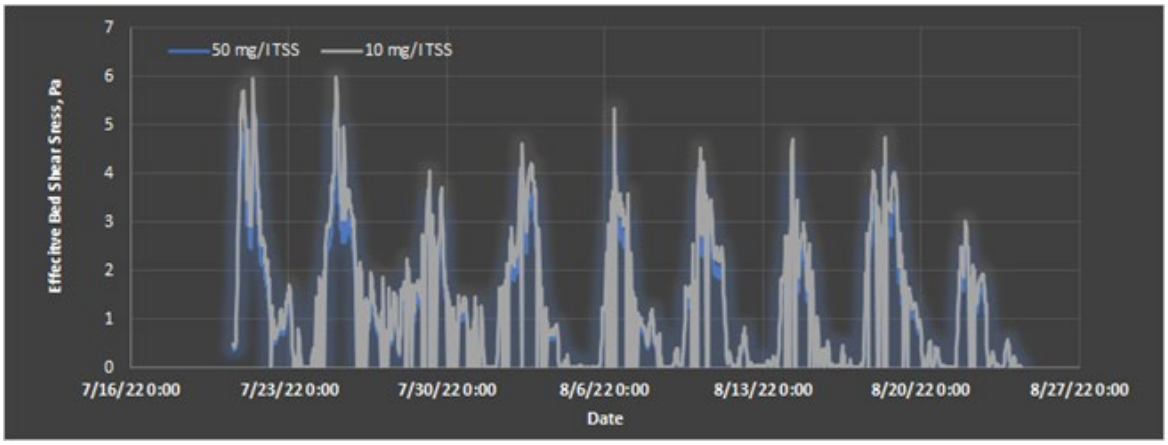

5. CONCLUSIONS

Based on historic bathymetric surveys, the 6 ft contour line is very stable both at the east and west ends of the proposed fiber optic cable route which indicates that there is not much erosion happening in the nearshore area of the South Bay. This supports the decision that a buried cable at 3 ft to 6 ft will not result in scouring and exposure of the buried cable.

A recent study a few kilometers south of the proposed cable route in a shallow water depth of 1.5 m shows that the combined effect of winds and currents results in bursts of erosion in which sediments get carried away by the tidal currents in the water column.

However, the field study also showed cycles of erosion and deposition bursts resulting in small oscillations in the bed level (changing up or down by a few centimeters).

A simplified sediment transport analysis performed using the Sedtrans05 tool also shows periods of erosion and deposition with erosion increasing with wave heights. Deposition depends on the availability of total suspended sediments in the water column from both freshly eroded mass as well as coming from other regions.

There is a small incremental / decremental change in the wave heights and currents for the year 2050 due to climate change and this should not exacerbate erosion or deposition processes.

Based on the analysis ERM anticipates that will not be any significant scour/erosion to expose the buried cable based on current or climate change scenarios over a 30 yr timeline

6. REFERENCES

A2Sea. 2022. *Acoustic Doppler Current Profiler (ADCP) Current Data*. San Francisco Bay Cable Route Survey. P2036-SFB-RES-3. Issue 04. 2023, January 24th.

Barnard, P., D. H. Schoellhamer, B.E. Jaffe, L.J. McKee. 2013. Sediment transport in the San Francisco Bay Coastal System: An Overview. Marine Geology. Volume 345, November 1, 2013, Pages 3-17. [https://doi.org/10.1016/j.margeo.2013.04.005].

Egan, G., G. Chang, S. McWilliams, G. Revelas, O. Fringer, S. Monismith. 2020. Cohesive Sediment Erosion in a Combined Wave-Current Boundary Layer in a Combined Wave-Current Boundary Layer. Journal of Geophysical Research-Oceans. Volume 126. Issue 2. December 2020.

Jaffe, B.E and A.C. Foxgrover. 2006[a]. A History of intertidal flat area in South San Francisco Bay, California: 1858 to 2005, U.S. Geological Survey Open-File Report 2006-1262, 32 pp. [URL: http://pubs.usgs.gov/of/2006/1262]

Jaffe, B.E and A.C. Foxgrover. 2006[b]. Sediment Deposition and Erosion in South San Francisco Bay, California from 1956 to 2005. U.S. Geological Survey Open-File Report 2006-1287, 24 pp. [URL: http://pubs.usgs.gov/of/2006/1287]

O'Neill, A. C., L.H. Erikson, P.L. Barnard, 2017. Downscaling Wind and Wavefields for 21st Century Coastal Flood Hazard Projections in a Region of Complex Terrain. American Geophysical Union Advancing Earth and Space Science. Volume 4, Issue 5, pp. 314-334. May 2017

Neumeier, U., C.F. Ferrarin, C.L. Almos, G. Umgiesser, M.Z. Li, 2008. Sedtrans05: An Improved Sediment-Transport Model for Continental Shelves and Coastal Waters with a New Algorithm for Cohesive Sediments. Computers & Geosciences, pp. 1223-1242, Volume 34, 2008. [doi:10.1016/j.cageo.2008.02.007]

Woodrow, D. L., T. A. Fregoso, F. L. Wong and B. Jaffe, 2014. Late Holocene Sedimentary Environments of South San Francisco Bay, California, Illustrated in Gravity Cores. Open-File Report 2014-1198. U.S. Department of the Interior, U.S. Geological Survey. 97 pages, 2014. [Late Holocene Sedimentary Environments of South San Francisco Bay, California, Illustrated in Gravity Cores (usgs.gov)]